

COMPUTED VARIOMETER RESPONSE  
TO ELEVATOR MOTION AND THERMALS

by

Malcolm J. Abzug  
Pacific Palisades  
California, USA

Presented at the XV OSTIV Congress  
Rayskala, Finland, 1976

ABSTRACT

The operating characteristics of different types of variometers are investigated by computing their responses under typical sailplane operating conditions. Variometer system equations of motion are generated from the equations of their elements. These equations are solved together with the nonlinear equations of motion of a typical sailplane, for both elevator motion and thermal inputs. The results show that both venturi and diaphragm type compensated variometers reduce greatly the rate of climb indications due to stick motions. Increased lag in the variometer system and a modification reducing the total energy correction both result in poorer performance. The compensated variometers operate essentially without lag when a thermal is encountered.

INTRODUCTION

Flight test measurements of the performance of sailplane instruments are subject to problems similar to those encountered in flight test measurements of sailplane performance. That is, unless the air is quite still and the test procedure is sophisticated, experimental errors are large compared with the quantities of interest. The availability of efficient digital computer programs for integrating the equations of motion of the sailplane and its instruments opens the possibility of getting comparisons of various instrument system concepts under rigidly controlled conditions. In addition, improved understanding of instrument dynamics can be obtained from details of the solutions. This approach is applied in this paper to uncompensated and total-energy compensated variometer systems. Instrument installation errors and in particular angle of attack effects on measured

static pressure are not treated. These errors are important in variometer dynamic performance, but their effects are additive to those developed in this paper, and can be analyzed at a later time. Time lags due to long pressure supply lines are in the same category.

VARIOMETER SYSTEM ELEMENTS

The differential equations that describe the dynamics of sailplane variometer systems are obtained by combining the equations of certain elements common to these systems. These elements are the laminar-flow restriction, the spring-loaded diaphragm, the insulated flask, and the flow indicator. Schematic sketches of these elements and their corresponding differential equations are given in Figures 1 through 4. In all of these figures

$C$  = constant of proportionality

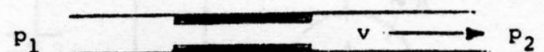
$p$  = pressure

$R$  = instrument reading

$v$  = flow velocity

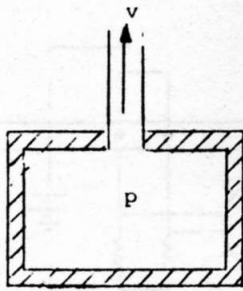
$V$  = volume

$\rho$  = density



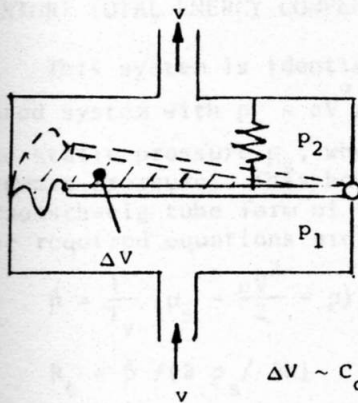
$$v = C_r (P_1 - P_2), \text{ Poiseuille or laminar flow}$$

FIGURE 1. - THE LAMINAR FLOW RESTRICTION



$v = -C_f \dot{p}$  , adiabatic process  
 $p\rho^\gamma = \text{constant}$   
 $v$  is proportional to  $\dot{p}$

FIGURE 2. - THE INSULATED FLASK



$\Delta V \sim C_d (p_1 - p_2)$   
 $\dot{v} \sim v = C_d (\dot{p}_1 - \dot{p}_2)$

FIGURE 3. - THE SPRING-LOADED DIAPHRAGM

#### UNCOMPENSATED VARIOMETER SYSTEM

Three variometer elements are assembled to form an uncompensated variometer system, as shown in Figure 5. From the equations on Figures 1, 2, and 4

$v = -C_f \dot{p}$  (1)  
 $R_u = C_v v$  (2)  
 $v = C_r (p - p_s)$  (3)

combining equations (1) and (3)

$$\dot{p} = \frac{1}{T_v} (p_s - p) \quad (4)$$

where the system time constant

$$T_v = C_f / C_r \quad (5)$$

The remaining proportionality constant  $C_v$  is found from the steady instrument response to a ramp input in static pressure  $p_s = \alpha t$ , where  $\alpha$  is a constant and  $t$  is the time. The solution of equation (4) as time goes to infinity is

$$\dot{p} = \dot{p}_s = (\partial p_s / \partial h) \dot{h} = \alpha, \quad t \rightarrow \infty \quad (6)$$

The reading of a properly calibrated variometer will approach the altitude rate  $\dot{h}$  under these conditions.

Thus,

$$R_u = \dot{h} = -C_f C_v \dot{p} = -C_f C_v (\partial p_s / \partial h) \dot{h}, \quad t \rightarrow \infty \quad (7)$$

$$\text{and } C_f C_v = -1 / (\partial p_s / \partial h) \quad (8)$$

Returning to the general equations (1) and (2) and using equation (8)

$$R_u = \dot{p} / (\partial p_s / \partial h) \quad (9)$$

Equations (4) and (9) are the desired (first order) differential and output equations of the uncompensated variometer.

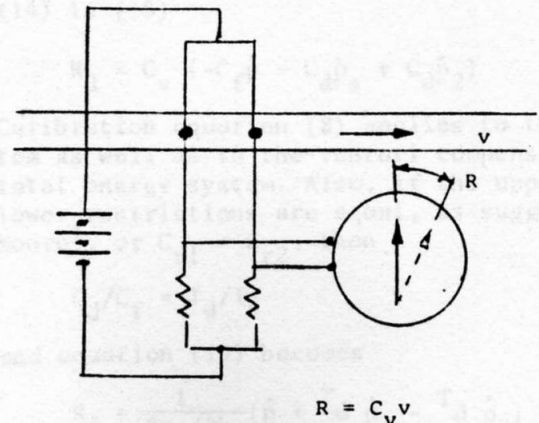


FIGURE 4. - THE (THERMISTOR BRIDGE) FLOW INDICATOR

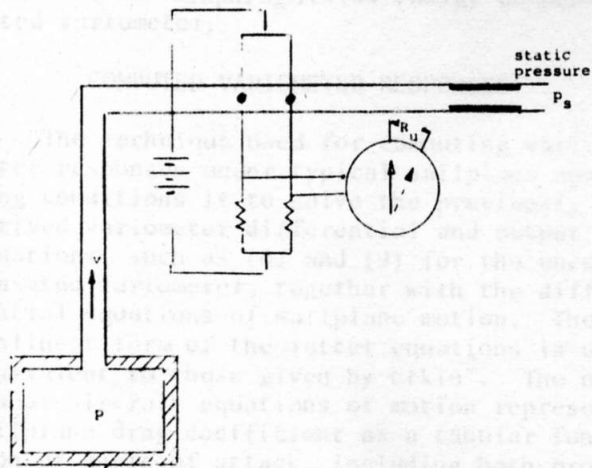


FIGURE 5. - UNCOMPENSATED VARIOMETER SYSTEM

#### VENTURI TOTAL ENERGY COMPENSATED VARIOMETER

This system is identical to the uncompensated system with  $p_s - \rho v^2/2$  substituted for the static pressure  $p_s$ , where  $\rho v^2/2$  is the dynamic pressure. This holds true for the Braunschweig tube form of this system as well. The required equations are

$$\dot{p} = \frac{1}{T_v} (p_s - \frac{\rho v^2}{2} - p) \quad (10)$$

$$R_t = \dot{p} / (\partial p_s / \partial h) \quad (11)$$

#### DIAPHRAGM TOTAL-ENERGY COMPENSATED VARIOMETER SYSTEM

Following Moore<sup>1</sup> the diaphragm total energy system is shown in Figure 6.

From the equations on Figures 1 through 4

$$v_1 = -C_f \dot{p} \quad (12)$$

$$v_2 = C_{r2} (p_2 - p_t) \quad (13)$$

$$v_2 = C_d (\dot{p}_s - \dot{p}_2) \quad (14)$$

$$R_d = C_v v_3 = C_v (v_1 - v_2) \quad (15)$$

where  $R_d$  is the instrument reading. Also, from equation (4)

$$\dot{p} = \frac{1}{T_v} (p_s - p) \quad (16)$$

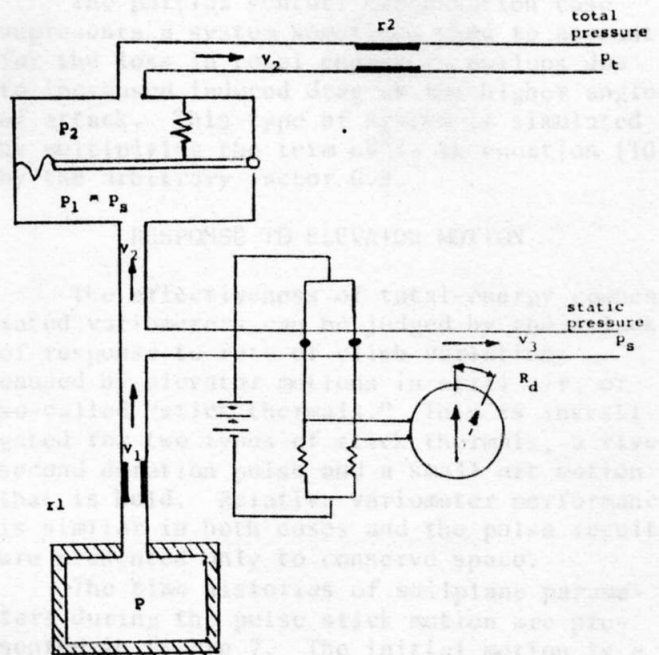


FIGURE 6. - DIAPHRAGM TOTAL-ENERGY COMPENSATED VARIOMETER SYSTEM

where  $T_v$  is the time constant of the flask and lower ( $r_1$ ) restriction. Equating (12) and (14)

$$\dot{p}_2 = \dot{p}_s + \frac{1}{T_d} (p_t - p_2) \quad (17)$$

where

$$T_d = C_d / C_{r2} \quad (18)$$

the time constant of the diaphragm and upper ( $r_2$ ) restriction. Using equations (13) and (14) in (15)

$$R_d = C_v (-C_f \dot{p} - C_d \dot{p}_s + C_d \dot{p}_2) \quad (19)$$

Calibration equation (8) applies to this system as well as to the venturi compensation total energy system. Also, if the upper and lower restrictions are equal, as suggested by Moore<sup>1</sup>, or  $C_{r1} = C_{r2}$ , then

$$C_d / C_f = T_d / T_v \quad (20)$$

and equation (19) becomes

$$R_d = \frac{1}{\partial p_s / \partial h} (\dot{p} + \frac{T_d}{T_v} \dot{p}_s - \frac{T_d}{T_v} \dot{p}_2) \quad (21)$$

Equations (16), (17), and (21) are the desired

(second-order) differential and output equations for the diaphragm total-energy compensated variometer.

#### COMPUTED VARIOMETER RESPONSES

The technique used for computing variometer responses under typical sailplane operating conditions is to solve the previously derived variometer differential and output equations, such as (4) and (9) for the uncompensated variometer, together with the differential equations of sailplane motion. The nonlinear form of the latter equations is used, equivalent to those given by Etkin. The nonlinear aircraft equations of motion represent sailplane drag coefficient as a tabular function of angle of attack, including both profile and induced drag. This is more complicated than the linearized equations of motion but since the total energy correction is a function of flight velocity squared, a precise evaluation requires the nonlinear equations of aircraft motion. Some details on the digital computer program that produces numerical solutions of the variometer system and sailplane equations are given in the Appendix. Five alternate variometer systems are analyzed, as listed in Table 1.

The partial venturi compensation case represents a system sometimes used to account for the loss in total energy in pullups due to increased induced drag at the higher angles of attack. This type of system is simulated by multiplying the term  $\rho V^2/2$  in equation (10) by the arbitrary factor 0.9.

#### RESPONSE TO ELEVATOR MOTION

The effectiveness of total-energy compensated variometers can be judged by their lack of response to rate of climb variations caused by elevator motions in still air, or so-called "stick thermals." This is investigated for two types of stick thermals, a five-second duration pulse and a small aft motion that is held. Relative variometer performance is similar in both cases and the pulse results are presented only to conserve space.

The time histories of sailplane parameters during the pulse stick motion are presented in Figure 7. The initial motion is a steady glide at an equivalent airspeed of 54.7 mph, with a descent rate of 160.8 feet per minute. The aft stick pulse lasts for four seconds and reaches a maximum incremental elevator angle of one degree. A rate of climb increment of 400 feet per minute is established

TABLE 1  
VARIOMETER SYSTEMS ANALYZED

System	Equations	Flask Time Constant $T_v$	Diaphragm Time Constant $T_d$	Other
Uncompensated	4, 9	0.5	-	-
Venturi Total-Energy Compensated	10, 11	0.5	-	-
Slow Response Venturi Total-Energy Compensated	10, 11	2.0	-	-
Partial Venturi Total-Energy Compensated	10, 11	0.5	-	0.9 of Full Compensation
Diaphragm Compensated	16, 17, 21	0.5	0.5	-

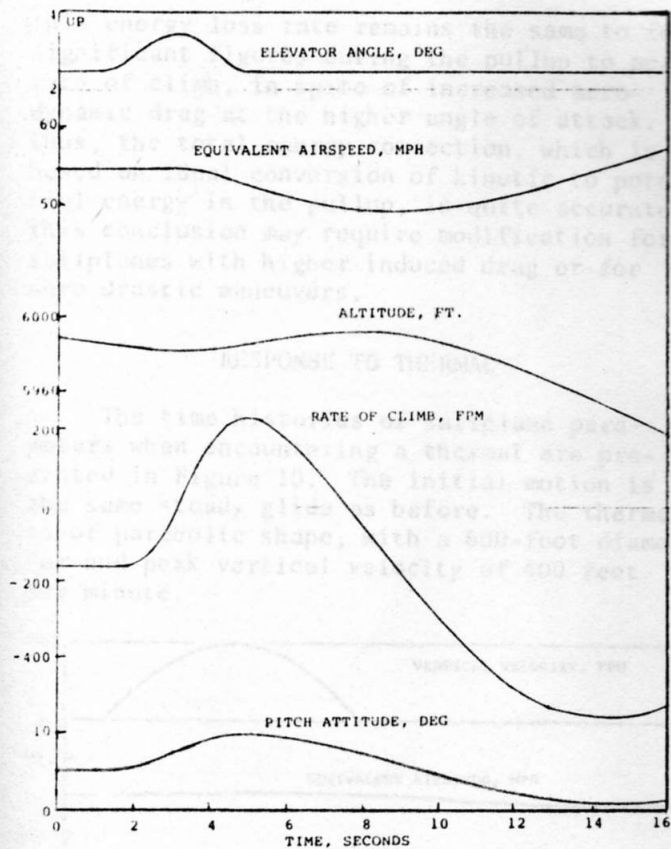


FIGURE 7. - CALCULATED SAILPLANE RESPONSE TO ELEVATOR PULSE

briefly. The ensuing motion is the well-known "phugoid" at essentially the initial angle of attack (not plotted).

The readings of the uncompensated and venturi total-energy variometer systems during this maneuver are compared with the true rate of climb in Figure 8. Aside from a slight time lag the uncompensated system indicates the true rate of climb. The initial indication looks like entry into a thermal, if the pilot is unaware of the slight stick motion. The venturi total-energy compensated system is quite effective in reducing the indicated rate of climb.

Four total-energy compensated systems are compared in Figure 9, at a larger vertical scale, for the same maneuver. The venturi and diaphragm systems have almost identical responses. A rate of climb error of 6.4 feet per minute occurs at 5 seconds, corresponding to the peak true rate of climb. This error is 1.6 percent of the rate of climb increment of 397 feet per minute. The partial venturi compensated system performs more poorly, with an error of 41.9 feet per minute at 5 seconds, or 10.6 percent. The slow-response venturi system

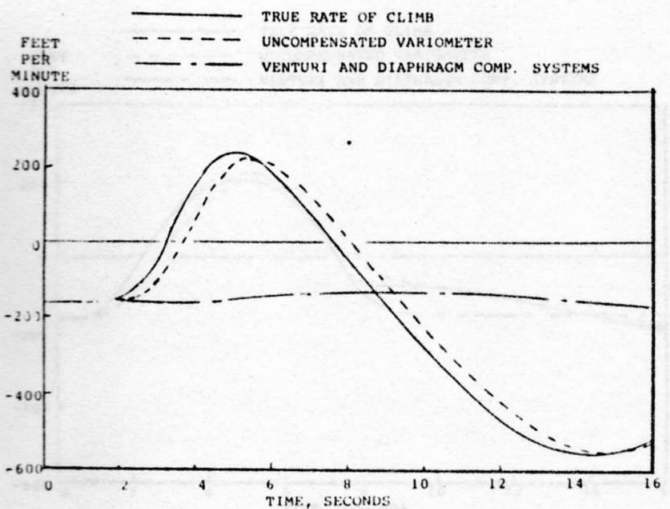


FIGURE 8. - COMPARISON OF VARIOMETER READINGS WITH TRUE RATE OF CLIMB DURING RESPONSE TO ELEVATOR PULSE

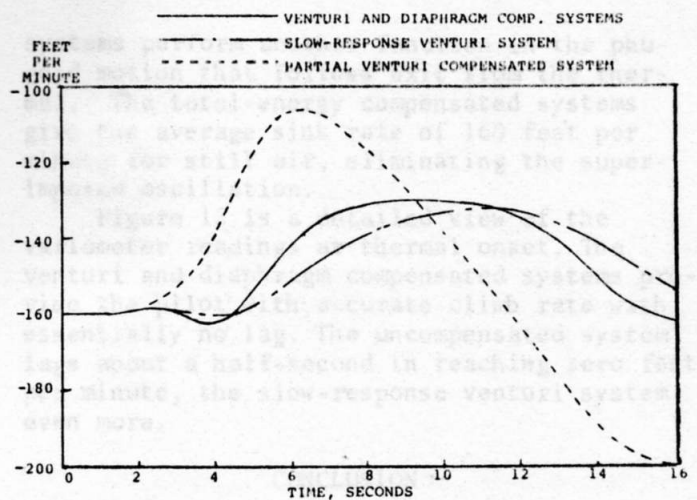


FIGURE 9. - COMPARISON OF COMPENSATED VARIOMETER SYSTEMS DURING RESPONSE TO ELEVATOR PULSE

behaves as expected, with response like that of the basic venturi system, but lagged in time.

The reason for the relatively good performance of the total-energy compensation systems for this case is found in the variation with time of the total (potential plus kinetic) energy for the sailplane. The total energy drops at a steady rate of 2190 pound-feet per second during the steady glide, due to drag.

This energy loss rate remains the same to four significant figures during the pullup to peak rate of climb, in spite of increased aerodynamic drag at the higher angle of attack. Thus, the total energy correction, which is based on ideal conversion of kinetic to potential energy in the pullup, is quite accurate. This conclusion may require modification for sailplanes with higher induced drag or for more drastic maneuvers.

#### RESPONSE TO THERMAL

The time histories of sailplane parameters when encountering a thermal are presented in Figure 10. The initial motion is the same steady glide as before. The thermal is of parabolic shape, with a 600-foot diameter and peak vertical velocity of 400 feet per minute.

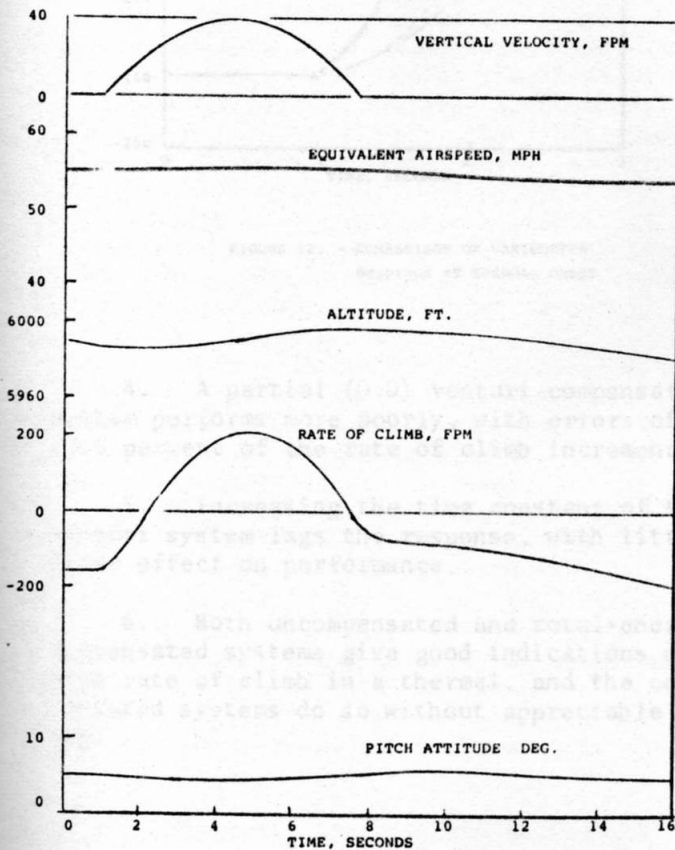


FIGURE 10. - CALCULATED SAILPLANE RESPONSE TO THERMAL

The readings of the uncompensated and total-energy compensated systems during this motion are compared with the true rate of climb in Figure 11. While both system types give reasonably good indications of the true rate of climb the total-energy compensated

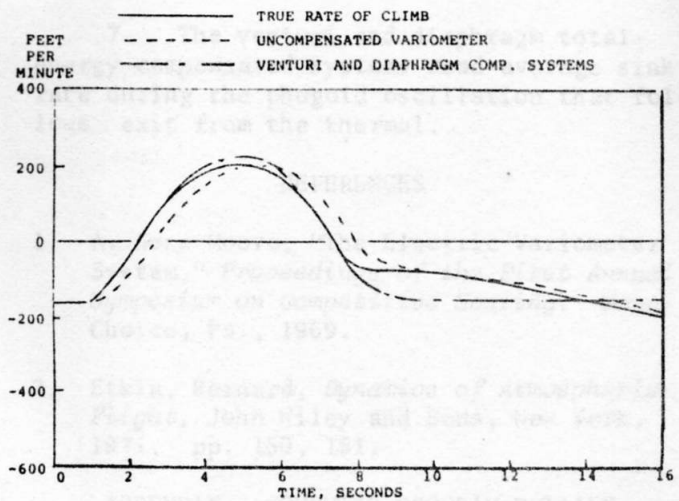


FIGURE 11. - COMPARISON OF VARIOMETER READINGS WITH TRUE RATE OF CLIMB DURING RESPONSE TO THERMAL

systems perform another function in the phugoid motion that follows exit from the thermal. The total-energy compensated systems give the average sink rate of 160 feet per minute for still air, eliminating the superimposed oscillation.

Figure 12 is a detailed view of the variometer readings at thermal onset. The venturi and diaphragm compensated systems provide the pilot with accurate climb rate with essentially no lag. The uncompensated system lags about a half-second in reaching zero feet per minute, the slow-response venturi system even more.

#### CONCLUSION

The following conclusions are drawn from this variometer response analysis:

1. Differential equations for the dynamics of sailplane variometers can be obtained by combining the equations of elements common to these systems.
2. When an aft stick pulse is applied during a steady glide the reading of an uncompensated variometer looks like entry into a thermal.
3. Both venturi and diaphragm total-energy compensated systems are effective in reducing the indicated rate of climb in stick thermals, producing errors of 1.6 percent of the rate of climb increment.

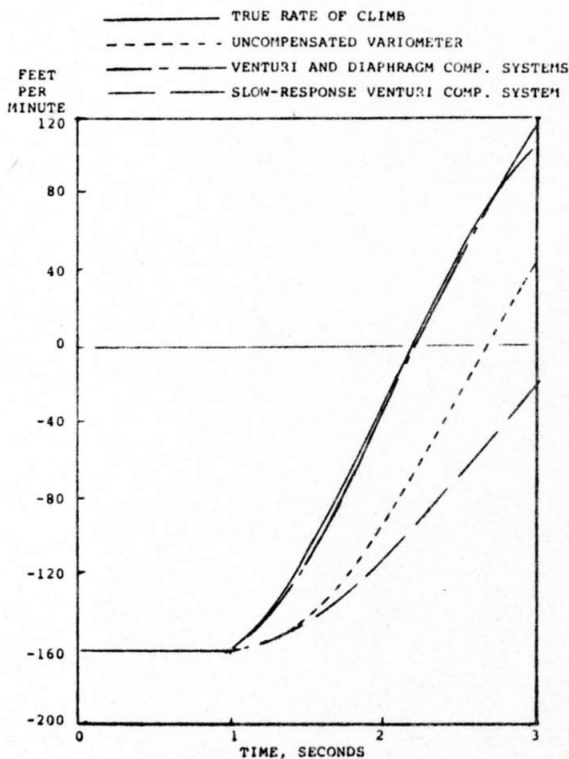


FIGURE 12. - COMPARISON OF VARIOMETER READINGS AT THERMAL ONSET

4. A partial (0.9) venturi compensation system performs more poorly, with errors of 10.6 percent of the rate of climb increment.

5. Increasing the time constant of the venturi system lags the response, with little other effect on performance.

6. Both uncompensated and total-energy compensated systems give good indications of true rate of climb in a thermal, and the compensated systems do so without appreciable lag.

7. The venturi and diaphragm total-energy compensated systems read average sink rate during the phugoid oscillation that follows exit from the thermal.

#### REFERENCES

1. A. Gene Moore, "The Electric Variometer System," *Proceedings of the First Annual Symposium on Competitive Soaring*. Manns Choice, Pa., 1969.
2. Etkin, Bernard, *Dynamics of Atmospheric Flight*, John Wiley and Sons, New York, 1971. pp. 150, 151.

#### APPENDIX - COMPUTER PROGRAM DETAILS

Aerodynamic and mass properties data used for the example sailplane are listed below, in the notation of Table 5.1 of Reference 2. The example sailplane is the Schweizer SGS 1-34 standard class machine.

Wing area = 151.08 sq. ft.

Reference chord = 3.24 ft.

Mass = 25.493 slugs

$I_Y = 800.0 \text{ slug-ft}^2$

$C_D = 0.01232 + .7627 \alpha^2$

$C_{L\alpha} = 6.028$

$C_{L\delta} = .3895$

$C_{m\alpha} = -0.6634$

$C_{m\delta} = -1.865$

$C_{Lq} = 5.427$

$C_{L\dot{\alpha}} = 1.222$

$C_{mq} = -24.82$

$C_{m\dot{\alpha}} = -5.321$

The nonlinear equations of aircraft motion and the variometer equations are solved on a general-purpose flight simulation digital computer program, using a CDC 6400 system. The program uses a fourth-order Runge-Kutta integration routine, with 0.02 second time intervals in this case.